Title: Lateral strength of nailed timber connections with decay

Type of article: Original article

Authors:

Kei Sawata

Affiliation: Research Faculty of Agriculture, Hokkaido University

Address: N9 W9, Sapporo 060-8589, Japan

Yoshihisa Sasaki

Affiliation: Research Faculty of Agriculture, Hokkaido University

Address: N9 W9, Sapporo 060-8589, Japan

Corresponding author:

Kei Sawata

Affiliation: Research Faculty of Agriculture, Hokkaido University

Address: N9 W9, Sapporo 060-8589, Japan

E-mail: ksawata@for.agr.hokudai.ac.jp

Telephone: +81 11-706-2528

FAX: +81 11-706-3636

Keywords: Yield theory; yield mode; brown rot fungus; member thickness; yield load

Footnote: none

Abstract

Loading tests were conducted on nailed connections with decay due to a brown rot fungus. The effect of the decay on the lateral strength of nailed connections was investigated. After loading tests, the sound and decayed regions of a nailed connection was observed in the cross section, which was cut parallel to the grain through the nailed point. The nailed connections with decay showed a low load during initial deformation when the main and side members had a decayed region in the boundary between them. The nailed connections showed low load after yielding when the sound region in the main member decreased. The yield load of nailed connections with decay was calculated based on the yield theory. The model of calculations had sound and decay regions within a member. The yield load of nailed connections obtained by the calculation based on the yield theory agreed with the results obtained by experiments when significant decay in a direction parallel to the grain was observed in the main and side members. This result indicates that the yield theory can estimate the yield load of nailed connections not only with a sound member but also a member that is partly or wholly decayed.

Introduction

Safety and serviceability are necessary functions of a structure, and those functions are often dependent on the stiffness and strength of the connections. The properties of the connections are required to persevere during its service period. Structural materials generally degrade as the service life increases. Wood is a material that is minimally affected by deterioration with age; however, it is affected by changes in humidity and may undergo biological deterioration under high humidity. One form of biological deterioration is decay. Decay causes a significant loss in the strength of the wood. The progress of decay differs with the direction of the grain and mycelium grows well along the longitudinal grain. Additionally, mycelial growth is not necessarily uniform within a wood. As a result, partial decay may happen in wood. When connections are decayed throughout, its properties would significantly degrade. However, for safety and serviceability of timber structures, it would be important to understand the properties of timber connections with part decay.

There has been a great deal of research on the strengths of wood exposed to a wood-decaying fungus [1]. The effects of decay on wood strength have been investigated for compressive strength [2, 3], tensile strength [4], bending strength [2, 5, 6], shear strength [2, 7], and hardness [2]. Although few studies have been conducted on timber connections with decay, reports have recently been increasing. Studies on timber connections with decay have been reported for dowelled connections [8] and nailed connections subjected to a lateral force. There have been several researches on the strengths of nailed connections exposed to a wood-decaying fungus. Studies on nailed connections have been conducted with side members composed of oriented strand board [9, 10], steel plate [11, 12], plywood, and medium density fiberboard [13]. These studies have indicated the decrease in strength of nailed connections caused by the decay.

Main and side members of nailed connections are composed of not only various materials but also various dimensions. The connection geometry has effects on a yield mode, which depends on a distribution of embedding stress in members and a yield bending moment of nail. Further, the nail length in the main member affects a withdrawal resistance in the main member. Consequently, the shape of the load–slip

curves of nailed connections, subjected to a lateral force, depends on the connection geometry [14]. There is little research that has examined the effects of decay on the strength of nailed connections with varying connection geometry. When decay is produced throughout main and side members, the strength of nailed connections will decrease because the embedding strength of wood [15] and withdrawal resistance in the main member [16] significantly decreases by decay. However, decay will not necessarily progress in a uniform manner within wood. Therefore, this study, conducted on the lateral loading tests of the decay-treated nailed connections with varying thicknesses of main and side members, investigated the effects of part decay in wood on the strength of nailed connections.

The strength of nailed connections with sound wood is often estimated by the calculation based on yield theory. The yield theory was developed by Johansen [17] and several standards have adopted it for the design of dowel-type timber connections subjected to lateral force [18, 19]. The estimation based on yield theory has been conducted on not only the single and double shear connections with fastener placed with its axis perpendicular to the surface of the member but also the connections with inclined screw [20], nailed connections with interlayer [21], connections with multiple slotted-in steel plates [22], and connections in solid wood panels with cross layers [23]. The yield theory has been applied to various connections subjected to lateral force. If the strength of nailed connections with part decay could be estimated by yield theory, it would be useful for the evaluation of safety of structures. Therefore, to estimate the strength of nailed connections with part decay, the nailed connections with members that had sound and decayed regions were modeled based on the yield theory and its suitability was investigated. The embedding tests were conducted on sound and decay-treated wood to obtain the embedding strength, which was used in the calculation.

Theory

The calculation of the strength of dowel-type connections subjected to lateral force is based on a theory originally proposed by Johansen [17]. In this theory, the embedding of wood and bending of dowel are

assumed to have perfect rigid plastic behavior, and several yield modes of the dowel-type connections are assumed. The yield mode is based on the hypothesis that the dowel remains straight during yielding, and the yield moment of the dowel is reached at several points. The strength of the dowel-type connections differs according to yield mode. This theory is also applied to the nailed connections [19, 24].

When the regions with different embedding strength were within a member, the dowel-type connections showed a greater number of yield modes than in the case with uniform embedding strength [25]. The reason is that, the yield mode varies according to the position of the plastic hinge and the rotation center of the dowel that rotate in the member. This study divided a member into two regions, which showed sound and decay status, because of modeling of nailed connections with part decay. In this case, main and side members each had five yield patterns as shown in Fig. 1. The yield mode of single shear nailed connections with part decay was decided by the combination of those patterns. Although the single shear nailed connections are well known to have six yield modes as shown in Fig. 2, when the main and side members were divided into two regions, the yield mode as shown in Fig. 2 was subdivided and the connections had eighteen yield modes as shown in Table 1.

The strength estimation equations of the nailed connections were derived from the equilibrium equations of forces and moments based on yield theory. The equations corresponding to yield modes that prevent the rotation of nails are expressed as follows:

$$P_{\mathrm{Ia}} = \left(f_{e11} \cdot t_{11} + f_{e12} \cdot t_{12}\right) \cdot d \quad (1)$$

$$P_{\mathrm{Ib}} = \left(f_{e21} \cdot t_{21} + f_{e22} \cdot t_{22}\right) \cdot d \quad (2)$$

where P_{Ia} and P_{Ib} are the values (N)corresponding to the mode Ia and Ib, respectively, f_{ei} (i=1, 2 and j=1, 2) is the embedding strength (N/mm^2) of the wood, t_{ij} (i=1, 2 and j=1, 2) is the distance (mm) as shown in Fig. 3, d is the nail diameter (mm).

When the nail is rotated in main and side members and the yield hinges are formed on nail, the moment of end of nail (Fig. 1) is

$$M_1 = \frac{1}{4}\left(A_1 \cdot P^2 + B_1 \cdot P + C_1\right) \quad (3)$$

$$M_2 = \frac{1}{4}\left(A_2 \cdot P^2 + B_2 \cdot P + C_2\right) \quad (4)$$

where M_1 and M_2 are moment, as shown in Fig. 1, and A_k, B_k, and C_k (k=1, 2) are coefficients, as shown in Table 2.

By $M_1+M_2=0$ in the boundary between main and side members, the equations corresponding to yield modes as shown in Table 1 are obtained as follows:

$$P = \frac{\sqrt{(B_1+B_2)^2 - 4(A_1+A_2)(C_1+C_2)} - (B_1+B_2)}{2(A_1+A_2)} \quad (5)$$

where P is the values corresponding to each yield mode and $P=P_{\mathrm{II}n}$, $P_{\mathrm{IIIa}n}$, $P_{\mathrm{IIIb}n}$, or $P_{\mathrm{IV}n}$ (n=1 to 4) (N), as shown in Fig. 2.

Using the values of $P_{\mathrm{II}n}$, $P_{\mathrm{IIIa}n}$, $P_{\mathrm{IIIb}n}$, or $P_{\mathrm{IV}n}$ which are the positive real number, the yield load of nailed connections (P_y) is obtained from following equation.

$$P_y = \min \begin{cases} P_{\mathrm{Ia}} \\ P_{\mathrm{Ib}} \\ P_{\mathrm{II}n} \\ P_{\mathrm{IIIa}n} \\ P_{\mathrm{IIIb}n} \\ P_{\mathrm{IV}n} \end{cases} \quad (n=1 \text{ to } 4) \quad (6)$$

Materials and methods

Nailed connection test

The strength of the nailed connections was determined from tests using solid lumbers, Japanese fir (*Abies sachalinensis*), used for the main and side members. The main and side members were 250 mm long and 45 mm wide. The side member thickness and nail length in the main member were of three types, as shown in Table 3. The distance from the point of the nail to the edge of the main member was 15 mm. Control and decay-treated specimens were prepared from the end-matched group. The average wood density of an end-matched small specimen without defects was 381 kg/m^3 (standard deviation: 41.0 kg/m^3) at an average moisture content of 7.67%. The main and side members had a nail lead hole of 3 mm diameter. The lead

147 hole was drilled before the main and side members were immersed in a water bath, which will be described
148 later. The main member was prepared with a hole of 25 mm diameter and 5 mm depth for the decay
149 procedure, as shown in Fig. 3.
150 Prior to the decay procedure, the wood samples were immersed in a water bath for more than 2 weeks to
151 increase their moisture content. The wood samples were placed in polyethylene bags with a filter and
152 sterilized by heating to 121 °C for 15 min. The hole for the decay procedure was filled with potato dextrose
153 agar and a small block covered with mycelium was placed in the potato dextrose agar. A small block of
154 Japanese fir was inoculated with a small piece of *Fomitopsis palustris* (Berk. et Curt.; a brown rot fungus)
155 on a mycelium mat, and the nutrient solution consisted of tap water, including 4% D-glucose, 0.3% peptone,
156 and 1.5% malt extract [7, 16]. The main and side members were assembled with paper strings and the lead
157 hole of the main member was aligned with that of the side member. The authors expected mycelial growth
158 to begin along the lead hole. The inoculated wood samples were incubated at 25 °C and 83% relative
159 humidity for 9 and 21 weeks.
160 When wood with decay is dried, the wood shows significantly shrinkage deformation. If the decay-treated
161 specimens are dried after decay procedure, the specimens might not be set up on testing equipment because
162 of the significant deformation. The strength of wood with moisture content above the fiber saturation point
163 is usually, almost, constant and the same observation has been obtained from the report for the embedding
164 strength of wood [15]. Therefore, to avoid the significant deformation and to increase moisture content up
165 to above the fiber saturation point, the wood samples were immersed in a water bath for more than 1 week
166 after the decay procedure. Control wood samples were also immersed in a water bath prior to the lateral
167 loading tests. The moisture content of the control and inoculated wood samples at the time of the lateral
168 loading tests were 70.3%–166% and 78.1%–279%, respectively.
169 Mycelium grows well under conditions of moisture content above the fiber saturation point, and the
170 exposure of nailed connections to high moisture encourages corrosion. When rust forms on the surface of
171 the nail shank, the surface roughness of the shank increases, therefore, nail corrosion leads to an increase in

172 strength of nailed connections. When the nail further corrodes, the nail shank decreases and the strength of
173 nailed connections are decreased [26]. The strength of nailed connections exposed to fungal attack is
174 affected by both wood decay and nail corrosion. In this study, the nails were driven into wood after the
175 decay procedure because the effects of rust on the nail on the strength of nailed connections were excluded,
176 and the effects of the decay were investigated.
177 The nails used in nailed connection tests were a CN65 nail having a nominal diameter of 3.33 ± 0.10 mm
178 and a nominal length of 63.5 ± 1.6 mm [27, 28]. A nominal length is the length from nail point to nail
179 head and the length of nail shank was 58 mm. The average bending strength corresponding to an angle of
180 45 degrees of the CN65 nail was obtained from the bending tests according to ISO 10984-1 [29], and was
181 1379 N/mm^2. The yield bending strength of the nails, according to EN12512 [30], was 599 N/mm^2. The
182 main and side members were connected with a nail after those were immersed in a water bath. The nails
183 were hand-driven into the radial direction to the annual ring of the main and side members and the nailed
184 connections were immediately tested after nailing. The nailed connections had three specifications that
185 differed with the thickness of the members. Each specification consisted of fifteen replicates. Five
186 specimens were control specimens and ten specimens were decay-treated specimens.
187 The main and side members of a nailed connection were loaded parallel to the grain as shown in Fig. 4(a).
188 The relative slips between the main and side members of the nailed connection were measured by two
189 displacement transducers. A load was applied up to a relative slip of 0.25 mm and, subsequently, was
190 reduced to 0 mm. This step was repeated three times. Then, a cyclic test was repeated three times to
191 produce the relative slips of 0.5, 0.75, 1.0, 2.0, and 4 mm. The slip level was determined from the load–slip
192 curves obtained from the preliminary loading tests of the nailed connections. The loading procedure was
193 adopted because the degradation of wood was investigated in the unloaded area of the nailed connection.
194 The tests were terminated when the load decreased to 60% of the maximum load or when the relative slip
195 reached 40 mm.
196 Embedding test

The dimensions of the embedding test specimens, which were cut from Japanese fir solid lumber, were 95 mm long, 45 mm wide, and 12 mm thick. Control and decay-treated specimens were prepared from the end-matched group. The average wood density of a specimen before decay procedure was 387 kg/m^3 (standard deviation: 17.1 kg/m^3) at an average moisture content of 12.7%. The nail used was a CN65 nail, a nail lead hole was 3 mm diameter, and the end distance was 20 mm.

The specimens were sterilized and placed in a polypropylene container containing the fungus culture of *Fomitopsis palustris*. Nutrient solution was tap water containing 4% D-glucose, 0.3% peptone, and 1.5% malt extract. The incubation was performed at 25 °C and 83% relative humidity for 6, 9, and 12 weeks. The embedding test specimens were immersed in a water bath for more than 1 week prior to the loading tests to avoid significantly shrinkage deformation, as described above. The moisture content of the control and inoculated specimens at the time of the loading tests were 120%–154% and 178%–273%, respectively.

After the above procedure, CN65 nails were hand-driven into the radial direction to the annual ring of the specimens and the embedding tests were immediately carried out after nailing. The monotonic loading tests parallel to the grain were carried out, as shown in Fig. 4(b). The tests were terminated when the load decreased to 60% of the maximum load or when the slip reached more than 3.5 mm. The control specimens were twelve and the decay-treated specimens were eighteen.

Results and discussion

Embedding strength

Figure 5 shows the representative embedding stress–displacement curves of the embedding specimens that had different degrees of decay. The mass loss was calculated from the weight of end-matched control and decay-treated specimens after embedding tests as follows:

$$ML = \frac{W_{CO} - W_{DO}}{W_{CO}} \times 100 \quad (7)$$

where ML is the mass loss (%), W_{CO} is the weight of oven-dry control specimen (g), W_{DO} is the weight of oven-dry decay-treated specimen (g).

222 The control specimen show almost constant load after displacement of 2 mm. The decay-treated specimens
223 with mass loss of 14.8% and 16.3% show a increase in the load up to the termination of test and that with
224 mass loss of 29.9% and 33.6% show almost constant load after displacement of 2 mm. The former had both
225 of sound and decayed regions in the nailing point and the latter had only decayed region in the nailing point.
226 In this study, to obtain the embedding strength of sound and decay wood, the embedding strength was
227 defined as the maximum embedding stress up to 2 mm displacement.
228 Figure 6 shows the relations between the embedding strength and mass loss. When the mass loss was in the
229 range of 8% to 20%, the specimens showed a large variable of embedding strength. The specimens with
230 mass loss of greater than 20% showed significantly lower embedding strength than the control specimens.
231 The visual feature by decay was not clear during embedding test, however, a discoloration, shrinkage, and
232 collapse were obviously observed by seasoning after embedding test. The specimens with mass loss of
233 lower than 20% showed partly a discoloration, shrinkage, and collapse in the nailing point and all
234 specimens with mass loss of greater than 20% showed those visual features by decay in the overall nailing
235 point. Therefore, the embedding strength with mass loss of greater than 20% was defined as the embedding
236 strength of decay region in this study. The embedding strength of sound region, which was obtained from
237 the embedding tests of control specimens, was 18.3 N/mm^2 and that of decay region was 1.26 N/mm^2.
238 Decay pattern of nailed connection
239 After the loading tests, the nailed connections were cut parallel to the grain through the nailed point, and
240 were conditioned to air-dry humidity. Figure 7 shows the typical cross section of nailed connections after
241 the loading test. A discoloration, crack across to the grain, shrinkage, and collapse, which were caused by
242 decay, were observed in main and side members by seasoning. Some specimens produced decay throughout
243 wood members and others produced part decay in wood members. In the case of the specimens with the
244 part decay, a member was mostly distinguishable in two regions, which were the sound and decayed
245 regions. The sound and decayed regions parallel to the nail axis were measured to obtain the degree of
246 decay of nailed connections. Table 4 shows the length of sound and decayed regions of individual

specimens. Because the presence or absence of decay and the length of decayed region differed with the specimens, the specimens with various degrees of decay could be obtained.

Load–slip curve of nailed connection

Figure 8 shows the representative load–slip curves of the nailed connections that had different degrees of decay. The load of the S3M7 control specimen shows a linear increase up to the yield point and a continuous increase after yielding. The S3M7-2 specimen, which had a sound side member and a partly decayed main member, exhibits almost the same load–slip curve as the S3M7 control specimen. The S3M7-9 specimen, which had a sound side member and a main member with no sound region, shows a smooth increase in the load during the initial deformation and a slight increase after yielding. The S3M7-8 specimen had a side member with no sound region and a partly decayed main member. The S3M7-10 specimen had the side and main members with no sound region. These specimens show a low load at the initial deformation, with the load of the S3M7-10 specimen being smaller than that of the S3M7-8 specimen.

A sound nailed connection subjected to a lateral force will develop a mechanism as follows: An embedding stress in the main and side members is concentrated on the boundary between those members during the initial deformation [31]. Thereafter, a plastic hinge is produced on the nail and a nailed connection reaches a yielding condition. A nailed connection shows an increase in the load by increasing both the withdrawal resistance in the main member and the nail–head pull-through resistance in the side member after yielding. When the nailed connections of the S3M7 group had sound regions in the boundary between the main and side members, the connections showed a sharp increase in the load during the initial deformation. The connections showed a low load during the initial deformation when there was a small sound region in the boundary between the main and side members, and showed a low load after yielding when the main member had no sound regions. This is because the decay of the main member causes a decrease in the embedding strength and withdrawal resistance [16]. Support for this observation can be understood by the mechanism described above.

The S6M4-5 and S6M4-7 specimens had sound regions in the boundary between the main and side members. These showed a sharp increase in the load during the initial deformation. However, the shape of the load–slip curves of these specimens, after yielding, differed from that of the S6M4 control specimen, and showed a slight increase in the load after yielding. The S6M4-10 specimen, which had no sound region in the side member and a partly decayed main member, showed a low load at the initial deformation. The S6M4-8 specimen, which had no sound region in the boundary between the main and side members, showed a lower load, and had an uncertain yield point on the load–slip curve.

The S8M2-2 specimen, which had a sound side member and a partly decayed main member, exhibited almost the same load–slip curve as the S8M2 control specimen. The S8M2-5 specimen, which had a sound side member and the main member with no sound region, showed a low load at the initial deformation. The S8M2-8 specimen, which had no sound region in the boundary between the main and side members, showed a smaller load than the S8M2-5 specimen. The S8M2-10 specimen, which had no sound region in either of the main and side members, showed an even lower load than the S8M2-8 specimen. The nailed connections of the S6M4 and S8M2 group also showed a low load during the initial deformation, when the main and side members had a decayed region in the boundary between them, and the decrease of the sound region in the main and side members caused the decrease in the load after yielding.

Yield load

Slip of sound nailed connections subjected to a lateral force is increased in proportion to the load, and then the slip is largely increased regardless of a slight increase in the load. Yield could be defined as status that the inclination of load–slip curves is significantly changed. Figure 9 shows the envelope load–slip curves of sound nailed connections and the inclination of tangent of load–slip curves ($dP/d\delta$). Regardless of the specification of nailed connections, the value of $dP/d\delta$ showed a sharp decrease up to 1 mm of slip and a slight decrease after 2 mm of slip. This result could be interpreted to mean that the yield load will be in the range of 1 to 2 mm of slip. The authors searched for the method to determine yield load. The yield load of nailed connections with three specifications could be obtained from the method as follows: The straight line,

297 fit to the initial linear portion of load–slip curve, is shifted in the positive *x*-direction by one third of the nail
298 diameter, and yield load is defined as the intersection of this line and the load–slip curve. The initial
299 straight line was determined by the line that goes through the origin and the point on the curve
300 corresponding to slip of one tenth of the nail diameter. In this study, the yield load was determined using
301 this method based on the concept described above, although the yield load of connections made with
302 mechanical fastener are often determined according to EN12512 [30], and ASTM D-5652 [32]. When the
303 slip corresponding to yield load was calculated from the load–slip curves as shown in Fig. 9, that obtained
304 from the method in this study was 1.67 mm–1.72 mm. The slip corresponding to yield load obtained
305 according to EN12512 and ASTM D-5652 was 0.60 mm–0.94 mm and 0.55 mm–0.59 mm, respectively.
306 The slip corresponding to yield load evaluated according to EN12512 and ASTM D-5652 was in the range
307 which showed a sharp decrease of the value of $dP/d\delta$. To compare the values obtained from same
308 evaluation method, this method also applied to the calculation of yield load of decay-treated specimens.
309 When the nailed connections had no sound region in the boundary between the main and side members,
310 they showed a low load at both the initial and later deformations (Fig. 8). Therefore, the yield load was
311 compared with the length of sound region in the boundary between the main and side members and the
312 comparison was shown in Fig. 10. The specimens that had no sound region in the main and side members
313 showed significantly lower yield loads. When the specimens had the length of sound region in a range of 13
314 to 53 mm, they tended to show a smaller yield load as the length of sound region was decreased. However,
315 they showed a large variable of yield load. It is considered that the yield load of nailed connections with
316 part decay will be affected by not only the length of sound region in the boundary between the main and
317 side members, but also the mechanism of nailed connections subjected to lateral force.
318 Comparison to experiment
319 The calculation of yield load based on yield theory was conducted on the nailed connections with part
320 decay. The embedding strength of sound (18.3 N/mm^2) and decay (1.26 N/mm^2) regions were obtained
321 from the embedding tests. The distance (t_{ij}) used in calculation was based on the values shown in Table 4.

322 The yield moment (M_y) of the nails was the plastic section modulus ($d^3/6$) times the yield bending strength
323 (599 N/mm^2) described above.
324 Figure 11 shows the relations between yield load obtained in the experiments and those calculated from the
325 yield theory. The yield load of S8M2-3 specimens obtained in the experiments was larger than that
326 calculated from the yield theory. The S8M2-3 specimen had the decay in neighborhood of nailing point and
327 a little part of the region from nailing point was sound. Because the model in this study established
328 requirements that the embedding strength is not changed along parallel to the grain in the decay region, the
329 calculated values might be underestimated. However, the calculated yield load of the other specimens was
330 close to those obtained in the experiments. These results indicate that the equation, which is derived in this
331 study based on the yield theory, is useful for estimating the yield load of the nailed connection with partial
332 and whole decay.
333
334 Conclusions
335 Loading tests were conducted on nailed connections that were exposed to a brown rot fungus, *F. palustris*;
336 the connections differed according to three specifications based on combinations of different side member
337 thicknesses and nail lengths in the main member. The yield load of nailed connections with part decay was
338 calculated based on yield theory. The results obtained can be summarized as follows:
339 1. The relations between load and slip of nailed connections were significantly affected by the decay. The
340 nailed connections with decay showed a low load during the initial deformation when the main and side
341 members had a decayed region in the boundary between them. The decrease of the sound region in the
342 main member caused the decrease in the load after yielding.
343 2. The yield load of the nailed connections decreased as the length of sound region in the boundary between
344 main and side members was decreased; however, there showed large variable of yield load.
345 3. The model, which had sound and decay regions within a member, was constructed based on yield theory.
346 The yield load of nailed connection as calculated based on the yield theory agreed with the results obtained

experimentally when significant decay in the direction parallel to the grain was produced in members. This result indicates that the yield theory can estimate the yield load of nailed connections not only with a sound member but also with a partly and wholly decayed member.

Acknowledgements

The authors wish to thank Ms. Nozomi Saito, Hokkaido University, for her assistance in the decay treatment. This work was supported by JSPS KAKENHI Grant Number 26850107 and 17K07870.

References

[1] Wilcox W (1978) Review of literature on the effects of early stages of decay on wood strength. Wood Fiber 9: 252-7

[2] Mizumoto S (1966) The effect of decay caused by *Gloeophyllum trabeum* on the strength properties of Japanese red pine sap-wood. J Jap For Soc 48: 7-11

[3] Toole E (1971) Reduction in crushing strength and weight associated with decay by rot fungi. Wood Sci 3: 172-8

[4] Brown F (1963) A tensile strength test for comparative evaluation of wood preservatives. Forest Prod J September: 405-12

[5] Kennedy R (1958) Strength retention in wood decayed to small weight losses. Forest Prod J October: 308-14

[6] Curling S, Clausen C, Winandy J (2002) Relationships between mechanical properties, weight loss, and chemical composition of wood during incipient brown-rot decay. Forest Prod J July/August: 34-9

[7] Takanashi R, Ishihara W, Sawata K, Sano Y, Azuma T, Mori M, Koizumi A, Sasaki Y, Hirai T (2014) Fractography of shear failure surface of softwood decayed by brown-rot fungus. J Wood Sci 60: 186-93

[8] Sawata K, Sasaki T, Doi S, Iijima Y (2008) Effect of decay on shear performance of dowel-type timber joints. J Wood Sci 54: 356-61

372 [9] Kent S, Leichti R, Rosowsky D, Morrell J (2004) Effects of wood decay by *Postia placenta* on the
373 lateral capacity of nailed oriented strand board sheathing and Douglas fir framing members. Wood Fiber
374 Sci 36: 560-72
375 [10] Kent S, Leichti R, Rosowsky D, Morrell J (2005) Effects of decay on the cyclic properties of nailed
376 connections. J Mater Civil Eng September/October: 579-85
377 [11] Toda M, Mori M, Ohashi Y, Hirai T (2010) Effects of wood decay on the shear performance of nailed
378 timber joint (in Japanese). Mokuzai Gakkaishi 56: 41-7
379 [12] Mori T, Tanaka K, Nakahata T, Kawano K, Yanase Y, Kurisaki H (2014) Estimation of shear strength
380 of nail driven into decayed wood. In: World Conference on Timber Engineering, Quebec City, Canada
381 [13] Toda M, Mori M, Takahashi H, Karimata T, Hirai T (2013) Effect of decay in structural wooden panels
382 on the shear performance of nailed timber joints (in Japanese). Mokuzai Gakkaishi 59: 152-61
383 [14] Sawata K, Honda K, Hirai T, Koizumi A, Sasaki Y (2010) Effect of member thickness and nail length
384 projecting from main member on shear performance of single shear nailed joints (in Japanese). Mokuzai
385 Gakkaishi 56: 317-25
386 [15] Sawata K, Takiuchi H, Toda M, Sasaki T, Mori M (2008) Effect of wood decay on embedding
387 performance of wood and shear performance of dowel-type joints and nailed joints. In: World Conference
388 on Timber Engineering, Miyazaki, Japan
389 [16] Takanashi R, Sawata K, Sasaki Y, Koizumi A (2017) Withdrawal strength of nailed joints with decay
390 degradation of wood and nail corrosion. J Wood Sci 63: 192-8
391 [17] Johansen K (1949) Theory of timber connections. In: International association for bridge and structural
392 engineering (IABSE) Pub 9: 249-62
393 [18] EN 1995-1-1 (2004) Eurocode 5 - design of timber structures - general common rules and rules for
394 buildings. European Committee for Standardization (CEN), Brussels
395 [19] AWC (2015) National design specification for wood construction with commentary. American Wood
396 Council, Leesburg, VA

397 [20] Bejtka I, Blass H (2002) Joints with inclined screws. In: 35th Meeting of CIB-W18, Kyoto, Japan
398 [21] Johnsson H, Lukaszewska E, Stehn L (2004) Nailed timber joints with a thick interlayer. In: World
399 Conference on Timber Engineering, Lahti, Finland
400 [22] Sawata K, Sasaki T, Kanetaka S (2006) Estimation of shear strength of dowel-type timber connections
401 with multiple slotted-in steel plates by European yield theory. J Wood Sci 52: 496-502
402 [23] Uibel T, Blass H (2006) Load carrying capacity of joints with dowel type fasteners in solid wood
403 panels. In: 39th Meeting of CIB-W18, Florence, Italy
404 [24] Standard for structural design of timber structures (2006) Architectural Institute of Japan, Tokyo, Japan,
405 pp 266-278
406 [25] Sawata K, Kawamura H, Takanashi R, Ohashi Y, Sasaki Y (2016) Effects of arrangement of steel
407 plates on strength of dowel-type cross laminated timber joints with two slotted-in steel plates subjected to
408 lateral force. In: World Conference on Timber Engineering, Vienna, Austria
409 [26] Ishiyama H, Koshihara M (2009) Experimental study on the performance of the nailed joint with the
410 rust (in Japanese). J Struct Constr Eng 74: 2281-2289
411 [27] JIS A 5508 (2009) Nails (in Japanese). Japanese Industrial Standard, Tokyo, Japan,
412 [28] JIS G 3532 (2011) Low carbon steel wires (in Japanese). Japanese Industrial Standard, Tokyo, Japan
413 [29] ISO 10984-1 (2009) Timber structures - Dowel-type fasteners - Part 1: Determination of yield moment.
414 ISO, Switzerland
415 [30] EN12512 (2002) Timber structures - Test methods - Cyclic testing of joints made with mechanical
416 fasteners. European Committee for Standardization (CEN), Brussels
417 [31] Sawata K, Shibusawa T, Ohashi K, Castellanos J, Hatano Y (2008) Effects of density profile of MDF
418 on stiffness and strength of nailed joints. J Wood Sci 54: 45-53
419 [32] ASTM D-5652 (1995) Standard test methods for bolted connections in wood and wood-based products.
420 American Society for Testing and Materials, West Conshohocken, PA, USA
421

422 Figure legends

423

424 Fig. 1. Yield pattern of main and side members.

425 f_{e11}, f_{e12}, f_{e21}, and f_{e22}, embedding strength corresponding to sound and decay status; t_{11} and t_{12}, region with

426 different status of side member; t_{21} and t_{22}, region with different status of main member; M_1 and M_2,

427 moment; M_y, yield moment; P, load

428 Fig. 2. Yield mode of nailed connection.

429 Fig. 3. Configuration of nailed connection specimen.

430 Fig. 4. Setup of lateral loading tests for nailed connection and embedding tests.

431 Fig. 5. Relationship between the embedding stress and displacement.

432 ML, mass loss

433 Fig. 6. Relationship between embedding strength and mass loss.

434 Fig. 7. Cross section of nailed connection after loading test.

435 [S], sound status; [D], decay status

436 Fig. 8. Relationship between the load and slip of nailed connections.

437 Fig. 9. Inclination of tangent of load–slip curves.

438 Fig. 10. Relationship between yield load and sound distance in boundary between main and side members.

439 *Open circles*, control specimens of S3M7; *filled circles*, decay-treated specimens of S3M7; *open triangles*,

440 control specimens of S6M4; *filled triangles*, decay-treated specimens of S6M4; *Open squares*, control

441 specimens of S8M2; *filled squares*, decay-treated specimens of S8M2

442 Fig. 11. Comparison of results of the experiment with results calculated based on the yield theory.

443 *Symbols*, see Fig. 10

444

Table 1. Yield mode

Mode	Value	Yield pattern	
		Side member	Main member
Ia	P_{Ia}	m1-0	-
Ib	P_{Ib}	-	m2-0
II1	P_{II1}	m1-11	m2-11
II2	P_{II2}	m1-11	m2-12
II3	P_{II3}	m1-12	m2-11
II4	P_{II4}	m1-12	m2-12
IIIa1	P_{IIIa1}	m1-21	m2-11
IIIa2	P_{IIIa2}	m1-21	m2-12
IIIa3	P_{IIIa3}	m1-22	m2-11
IIIa4	P_{IIIa4}	m1-22	m2-12
IIIb1	P_{IIIb1}	m1-11	m2-21
IIIb2	P_{IIIb1}	m1-11	m2-22
IIIb3	P_{IIIb3}	m1-12	m2-21
IIIb4	P_{IIIb4}	m1-12	m2-22
IV1	P_{IV1}	m1-21	m2-21
IV2	P_{IV2}	m1-21	m2-22
IV3	P_{IV3}	m1-22	m2-21
IV4	P_{IV4}	m1-22	m2-22

For the *abbreviations* of yield pattern, see Fig. 1

Table 2. Coefficients of quadric equation for moment

Yield pattern	A_1	B_1	C_1
m1-11	I_{11}	$2d\cdot I_{11}(J_{11}-J_{12}+2f_{e11}\cdot t_{12})$	$d^2\cdot I_{11}(J_{12}^2-J_{11}^2)-2d\cdot J_{12}(t_{11}+t_{12})$
m1-12	I_{12}	$2d\cdot I_{12}(J_{11}+J_{12})$	$d^2\cdot I_{12}(J_{11}^2-J_{12}^2)-2d\cdot J_{11}(t_{11}+t_{12})$
m1-21	$2I_{11}$	$4(t_{12}-d\cdot I_{11}\cdot J_{12})$	$2d^2\cdot I_{11}\cdot J_{12}(J_{12}-f_{e11}\cdot t_{12})-4M_y$
m1-22	$2I_{12}$	0	$-4M_y$
Yield pattern	A_2	B_2	C_2
m2-11	I_{22}	$2d\cdot I_{22}(J_{22}-J_{21}+2f_{e22}\cdot t_{21})$	$d^2\cdot I_{22}(J_{21}^2-J_{22}^2)-2d\cdot J_{21}(t_{21}+t_{22})$
m2-12	I_{21}	$2d\cdot I_{21}(J_{21}+J_{22})$	$d^2\cdot I_{21}(J_{22}^2-J_{21}^2)-2d\cdot J_{22}(t_{21}+t_{22})$
m2-21	$2I_{22}$	$4(t_{21}-d\cdot I_{22}\cdot J_{21})$	$2d^2\cdot I_{22}\cdot J_{21}(J_{21}-f_{e22}\cdot t_{21})-4M_y$
m2-22	$2I_{21}$	0	$-4M_y$

$I_{ij}=1/(f_{eij}\cdot d)$, $J_{ij}=f_{eij}\cdot t_{ij}$

Table 3. Nailed connection tests specimen

Type	Side member		Main member	
	t_1(mm)	t_1/l_n	t_2(mm)	t_2/l_n
S3M7	20	0.34	38	0.66
S6M4	33	0.57	25	0.43
S8M2	45	0.78	13	0.22

Table 4. Length of sound and decayed regions of decay-treated specimens.

Specimens	Side member		Main member	
	t_{11} (mm)	t_{12} (mm)	t_{21} (mm)	t_{22} (mm)
S3M7-1	-	20[S]	38[S]	-
S3M7-2	-	20[S]	25[S]	13[D]
S3M7-3	-	20[S]	24[S]	14[D]
S3M7-4	-	20[S]	19[S]	19[D]
S3M7-5	-	20[S]	15[S]	23[D]
S3M7-6	-	20[S]	12[S]	26[D]
S3M7-7	-	20[S]	11[S]	27[D]
S3M7-8	-	20[D]	27[S]	11[D]
S3M7-9	-	20[S]	38[D]	-
S3M7-10	-	20[D]	38[D]	-
S6M4-1	-	33[S]	25[S]	-
S6M4-2	-	33[S]	25[S]	-
S6M4-3	-	33[S]	25[S]	-
S6M4-4	-	33[S]	25[S]	-
S6M4-5	-	33[S]	14[S]	11[D]
S6M4-6	-	33[S]	11[D]	14[S]
S6M4-7	-	33[S]	12[S]	13[D]
S6M4-8	27[S]	6[D]	25[D]	-
S6M4-9	23[D]	10[S]	12[S]	13[D]
S6M4-10	-	33[D]	13[S]	12[D]
S8M2-1	-	45[S]	13[S]	-
S8M2-2	-	45[S]	8[S]	5[D]
S8M2-3	-	45[S]	13[D]	-
S8M2-4	-	45[S]	13[D]	-
S8M2-5	-	45[S]	13[D]	-
S8M2-6	-	45[S]	13[D]	-
S8M2-7	23[D]	22[S]	13[S]	-
S8M2-8	34[S]	11[D]	13[D]	-
S8M2-9	-	45[D]	13[D]	-
S8M2-10	-	45[D]	13[D]	-

t_{11}, t_{12}, t_{21}, and t_{22}, see Fig. 1; S, sound status; D, decayed status

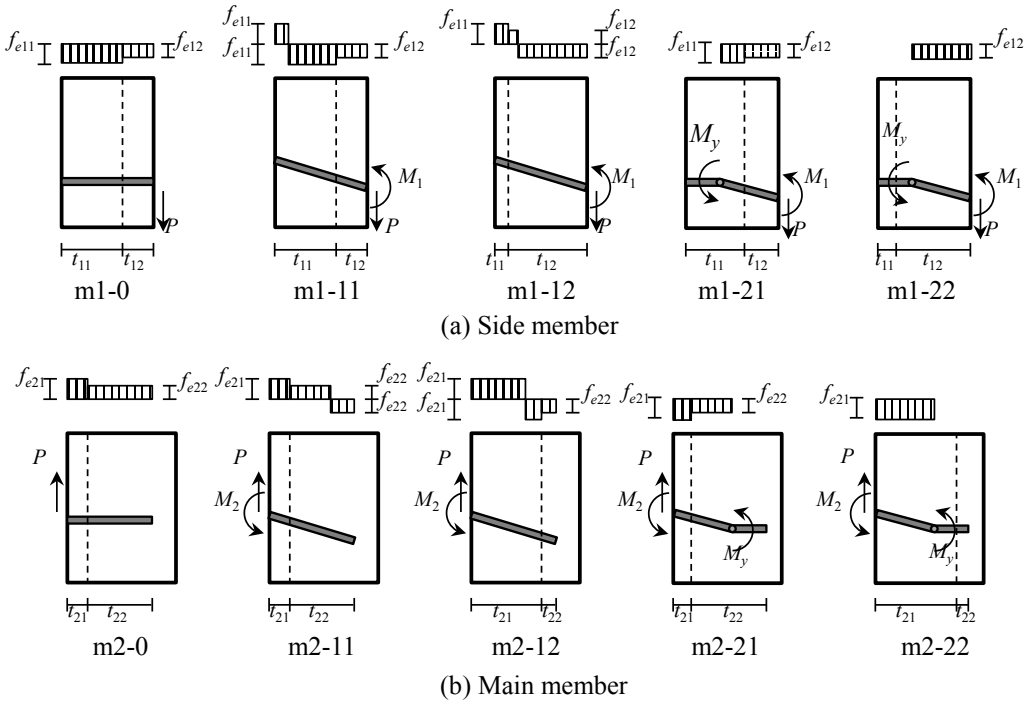

Fig. 1. Yield pattern of main and side members.

f_{e11}, f_{e12}, f_{e21}, and f_{e22}, embedding strength corresponding to sound and decay status; t_{11} and t_{12}, region with different status of side member; t_{21} and t_{22}, region with different status of main member; M_1 and M_2, moment; M_y, yield moment; P, load

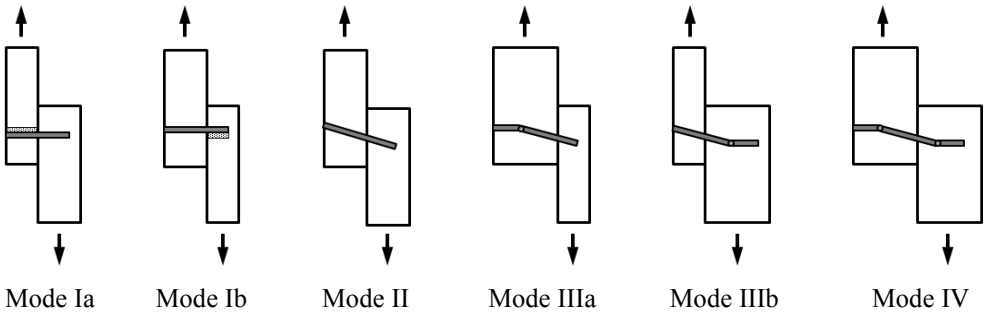

Fig. 2. Yield mode of nailed connection.

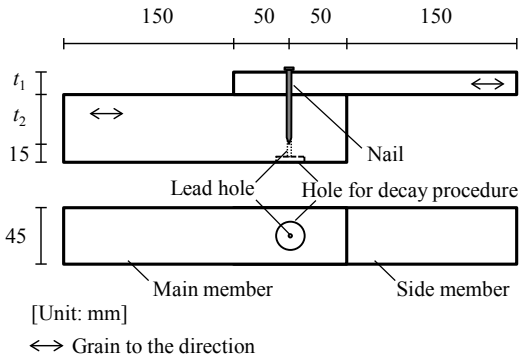

Fig. 3. Configuration of nailed connection specimen.

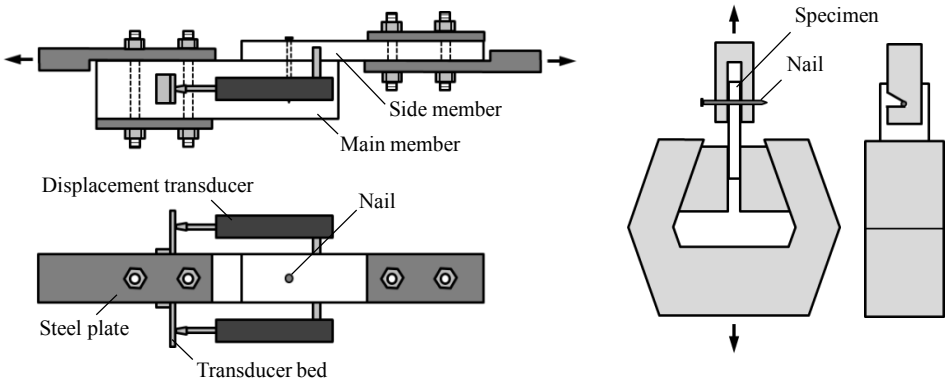

(a) Nailed connection test (b) Embedding test

Fig. 4. Setup of lateral loading tests for nailed connection and embedding tests.

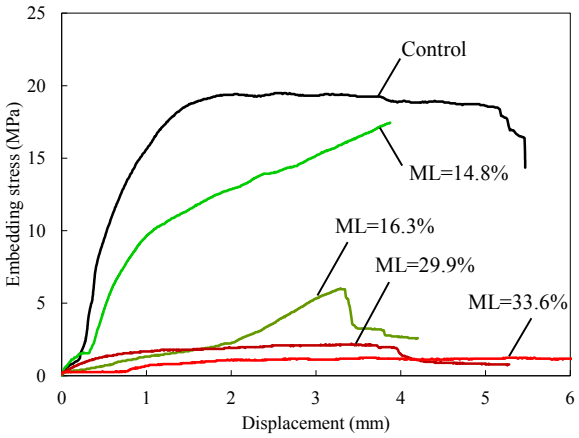

Fig. 5. Relationship between the embedding stress and displacement.

ML, mass loss

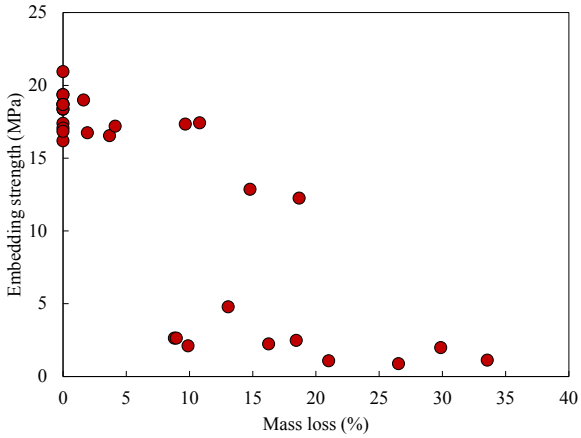

Fig. 6. Relationship between embedding strength and mass loss.

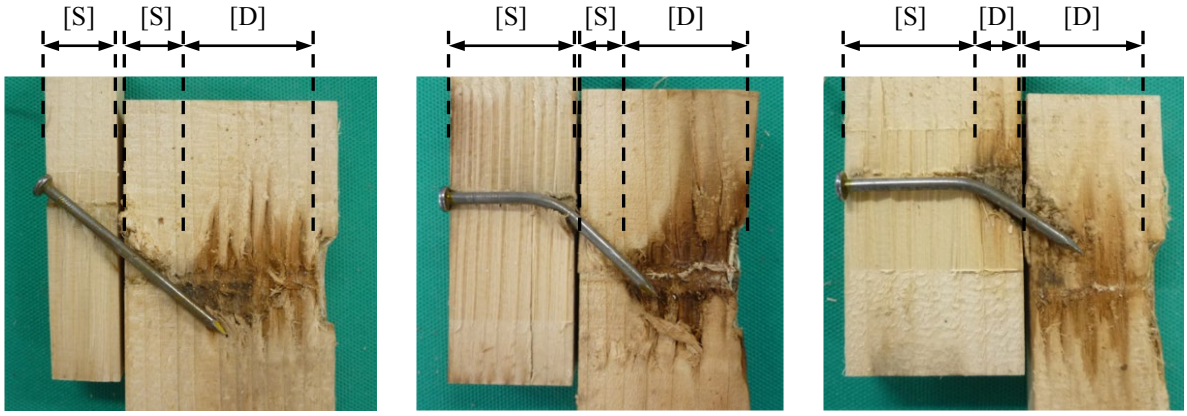

(a) S3M7-4 specimen (b) S6M4-7 specimen (c) S8M2-8 specimen

Fig. 7. Cross section of nailed connection after loading test.

[S], sound status; [D], decay status

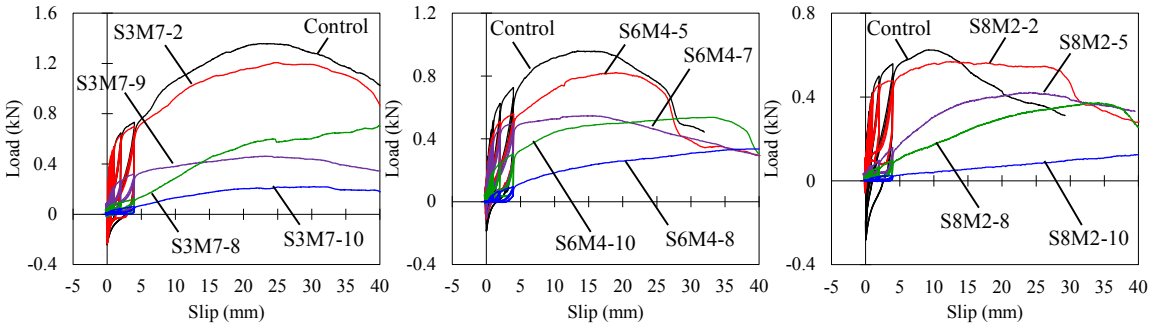

(a) S3M7 specimens (b) S6M4 specimens (c) S8M2 specimens

Fig. 8. Relationship between the load and slip of nailed connections.

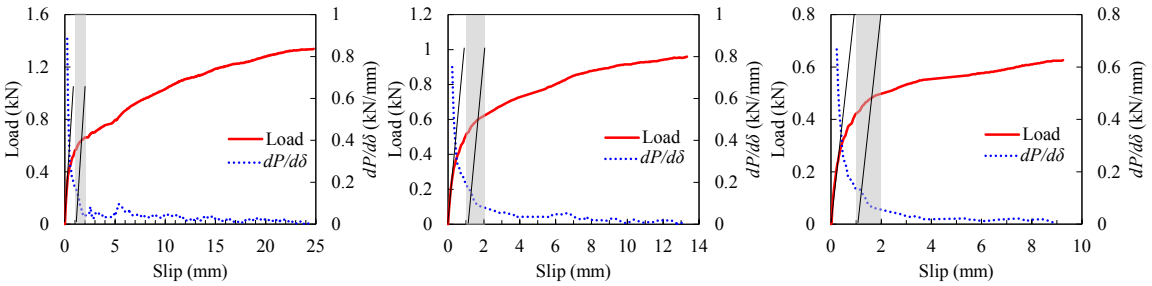

Fig. 9. Inclination of tangent of load–slip curves.

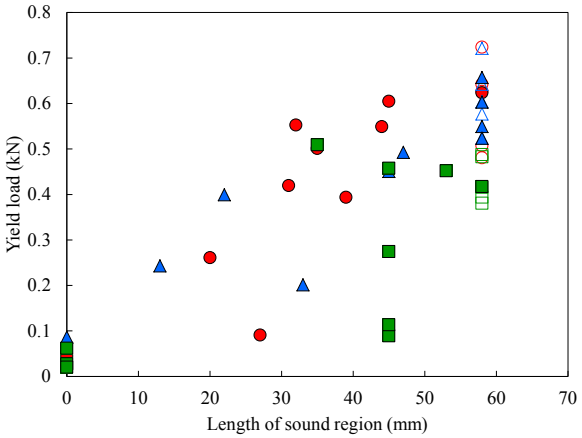

Fig. 10. Relationship between yield load and sound distance in boundary between main and side members.

Open circles, control specimens of S3M7; *filled circles*, decay-treated specimens of S3M7; *open triangles*, control specimens of S6M4; *filled triangles*, decay-treated specimens of S6M4; *Open squares*, control specimens of S8M2; *filled squares*, decay-treated specimens of S8M2

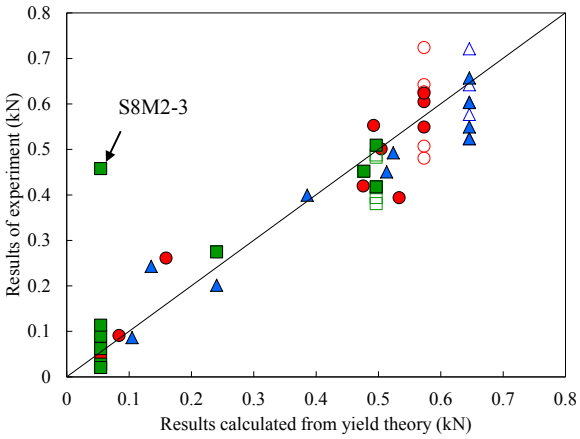

Fig. 11. Comparison of results of the experiment with results calculated based on the yield theory.

Symbols, see Fig. 10